RSC Advances

COMMUNICATION

View Article Online
View Journal | View Issue

Cite this: *RSC Adv.*, 2016, **6**, 62540

Received 23rd April 2016
Accepted 19th June 2016

DOI: 10.1039/c6ra10560b

www.rsc.org/advances

Deposition of hydroxyapatite–incorporated TiO_2 coating on titanium using plasma electrolytic oxidation coupled with electrophoretic deposition

Sviatlana A. Ulasevich,*[ab] Anatoly I. Kulak,[b] Sergey K. Poznyak,[c] Sergey A. Karpushenkov,[c] Aleksey D. Lisenkov[d] and Ekaterina V. Skorb[a]

A porous hydroxyapatite (HA)–incorporated TiO_2 coating has been deposited on the titanium substrate using a plasma electrolytic oxidation coupled with electrophoretic deposition (PEO-EPD). Potassium titanium(IV) oxalate is decomposed by micro arcs generated on the anode producing TiO_2 while HA particles have been simultaneously deposited on anode during EPD process. Hydroxyapatite and TiO_2 particles have been coagulated into roundish conglomerates with the average diameter in a range of 200–600 nm. The microstructure, as well as elemental and phase composition of the coatings have been examined by scanning electron microscopy (SEM), energy dispersive spectroscopy (EDS), glow discharge optical emission spectroscopy (GDOES), fourier transform infrared spectroscopy (FTIR) and X-ray diffraction (XRD). XRD has showed that the coatings are composed mainly of HA, rutile and anatase phases. The composition and surface morphologies are not strongly dependent on the applied voltages. The amount of HA deposited into the coating increases with increasing the applied voltage. The wear resistance of PEO-EPD coatings has been assessed using tribological tests. The bioactivity of the obtained coatings has been investigated in a simulated blood fluid.

Introduction

Titanium (Ti) and titanium alloys are frequently used as dental and orthopedic implant materials because of their excellent mechanical strength, chemical stability, and biocompatibility.[1] The biocompatibility of titanium is closely related to the properties of the surface oxide layer, in terms of its structure, morphology and composition. Thus far, a number of techniques have been developed to improve the surface properties of Ti implants such as plasma spraying, ion beam sputtering, chemical vapor deposition, dip coating, electrophoresis and electrochemical deposition.[2–4]

Plasma electrolytic oxidation (PEO) is one of the most useful methods for surface modification because it can produce porous and firmly adherent TiO_2 films on Ti implants.[5,6] This technique is based on a combined action of electrochemical anodic oxidation, high-voltage spark and a local high-temperature treatment. The high temperature at the breakdown sites and the high intensity of the electric field promote the appearance of noticeably nonequilibrium conditions and the involvement of the electrolyte components in the formation of the oxide coating. Advantages of this technique are the possibility to obtain well-adhered, firmly porous films on complex-shaped electrodes.[6,7]

Electrophoretic deposition (EPD) is another surface modification technique. It can be used to enhance the bioactivity of the surfaces by depositing of phosphate particles included in suspension toward the TiO_2 electrode surface under an applied electric field.[8,9] Advantages of this technique is short forming time, simplicity in instruments and the possibility to deposit stoichiometric, high purity coatings onto complex-shaped implants.[10–12] However, EPD technique does not provide high adhesion between the coating and substrate.[12,13]

Well-adhered coatings based on TiO_2 and biocompatible ceramic particles can be produced if EPD is combined with the PEO process (PEO-EPD).[13–20] It utilizes an electrolytic plasma to enhance the electrophoretic deposition process and improve adhesion.[13–15] This technique possesses all the advantages of wet coating methods and thus deposits the suspended particles on Ti alloy surfaces of various shapes and sizes without destroying their hydroxylated microstructure.[16–18] Furthermore, bioactive materials or antibiotics can be incorporated into the coating layer during the PEO-EPD process by tailoring the composition of the electrolyte solution.[19,20] For example, calcium and phosphate ions have been incorporated into the TiO_2 coating using an electrolyte solution containing calcium and phosphate sources.[2,5,13] More recently, well-crystallized hydroxyapatite (HA) particles together with TiO_2 coating have

[a]*Max Planck Institute of Colloids and Interfaces, Am Muhlenberg 1, 14424 Potsdam, Germany*

[b]*Institute of General and Inorganic Chemistry of NAS of Belarus, 220072 Minsk, Belarus*

[c]*The Research Institute for Physical Chemical Problems of the Belarusian State University, 220030 Minsk, Belarus*

[d]*Department of Materials and Ceramics Engineering, CICECO, University of Aveiro, 3810 193 Aveiro, Portugal*

been deposited. It has been revealed that a thin calcium phosphate layer has been directly deposited onto a plasma electrolytic oxidized Ti substrate. Calcium species have been confined to the surface regions either within the film, to a maximum depth of 18% of the film thickness, or as localized deposit on the film surface.[21,22]

Thus, it is still challenging to develop new methods that can allow the incorporation of bioactive materials, particularly in the form of crystalline phase, into the TiO_2 coating in an *in situ* manner.

In this study we suggest a new approach for uniform incorporation of HA particles into the TiO_2 coating on titanium during PEO-EPD process using an electrolyte based on potassium titanium(IV) oxalate and HA suspension. In particular, TiO_2 particles can be formed *via* the PEO process by decomposition of $K_2[TiO(C_2O_4)_2]$, while negatively charged HA particles migrate toward the Ti anode through the EPD process.

Experimental

Fabrication of HA–TiO_2 coatings

Plasma electrolytic oxidation coupled with electrophoretic deposition (PEO-EPD) was conducted under volt static conditions using a DC power supply with voltage and current ranges of 0–500 V and 0–3 A, respectively. The power supply provided constant voltage with an accuracy of about ±4% of the desired value. The single-compartment two-electrode electrochemical cell contained 200 mL of electrolyte. The temperature of the electrolyte was kept within a range of 25–50 °C using cold water circulating through a heat exchanger. The electrolyte was magnetically stirred to reduce temperature and concentration gradients in it.

Water–ethanol solution of 0.025 M calcium citrate $Ca_3(C_6H_5O_7)_2$, 0.025 M $K_2[TiO(C_2O_4)_2]$ and 0.006 M $Ca_{10}(PO_4)_6(OH)_2$ was prepared using commercial pure reagents and distilled water. HA suspension was synthesized from aqueous solutions of ammonium hydrophosphate and calcium chloride according the method suggested in ref. 23. The working electrode (anode) and the counter electrode were made of a titanium foil (≥99.7%). The anode area was 2 cm^2. The cathode area was approximately 2 times larger than that of the anode. Prior to plasma electrolytic oxidation, the electrodes were chemically polished in a mixture (2 : 1 by volume of HF : HNO_3) of concentrated HF (50 wt%) and HNO_3 (65 wt%) at 80 °C for 3–5 s, rinsed with distilled water and dried with air.

Structure characterization

X-ray diffraction (XRD) analysis was performed using an Advance D8 diffractometer (Bruker, Germany) with CuKα radiation in the range of 2θ from 10° to 60° at a scanning speed of 1°/min and a step size of 0.03°. FTIR spectra were taken at room temperature using a FTIR spectrometer (MIDAC 2000, USA) in a range of 400–4000 cm^{-1}. Scanning electron microscopy (SEM) was made using Hitachi S4100 and Hitachi SU-70 microscopes equipped with an energy-dispersive X-ray spectroscope (EDS) for morphological characterization of the sample surface. Thin layer of carbon was sputtered on the samples. Depth profiling analysis of the coatings was carried out by glow discharge optical emission spectroscopy (GDOES) using a HORIBA GD-Profiler 2 operating at a pressure of 650 Pa and a power of 30 W. The water contact angle value was measured at room temperature with an experimental angle error of ±1° using a Contact angle measuring system G10 (Kruss, Germany).

Tribological test

The dry sliding wear behavior of the PEO-EPD coatings was assessed with a Tribotec ball-on-disc oscillating tribometer. An AISI 52100 steel ball of 6 mm diameter was used as static friction partner at ambient conditions (25 ± 2 °C and 30% RH) under load in a range of 1–3 N with an oscillating amplitude of 10 mm and at a sliding velocity of 5 mm s^{-1}, for sliding distance of 12 m.

Bioactivity test

The bioactivity of the coatings was estimated by determination of the apatite formation ability in a simulated blood fluid (SBF) with ionic concentrations equal to human blood plasma. The SBF was prepared by dissolving reagent grade chemicals: KCl, NaCl, $NaHCO_3$, $K_2HPO_4 \cdot 3H_2O$, $MgCl_2 \cdot 6H_2O$, $CaCl_2$ and $NaSO_4$ according the method described by Kokubo and Takadama.[24] The pH was adjusted to 7.4 using 1 mol L^{-1} HCl and tris(hydroxymethyl)aminomethane (TRIS). The chemical composition was as follows (mmol L^{-1}): Na^+, 142.0; K^+, 5.0; Mg^{2+}, 1.0; Ca^{2+}, 2.5; Cl^-, 131.0; HCO_3^-, 5.0; HPO_4^{2-}, 1.0; SO_4^{2-}, 1.0. Plasma electrolytic coatings and Ti plate (as a reference sample) were immersed in 45 mL of the SBF solution at 37 °C for 21 days to induce apatite formation. The immersion media was updated every day. After the experiment, the samples were dried in air at room temperature and characterized using SEM.

Results and discussion

Fabrication of HA–TiO_2 coatings

A scheme of the experimental setup used for the PEO-EPD treatment is shown in Fig. 1a. According to preliminary results, $K_2[TiO(C_2O_4)_2]$ is decomposed by micro arcs generated on the anode, producing TiO_2 particles. The HA suspension was synthesized from alkali aqueous solutions (pH of the medium is 10.0–11.0), and HA particles in the suspension are negatively charged:[13]

$$Ca_{10}(PO_4)_6(OH)_2 + 2OH^- = Ca_{10}(PO_4)_6(O^-)_2 + 2H_2O.$$

Thus, HA particles migrate towards the Ti anode and become incorporated into the TiO_2 coating, resulting in the formation of HA–incorporated TiO_2 coating on the Ti surface. Analogously to the work,[25] ethanol is added to the electrolyte in order to retard the evolution of gas at the anode and prevent the destruction of the growing coating on the titanium surface. Calcium citrate has been added to inhibit the HA transformation into tricalcium phosphate during the PEO process. Furthermore, calcium citrate promotes the formation of uniform and homogeneous

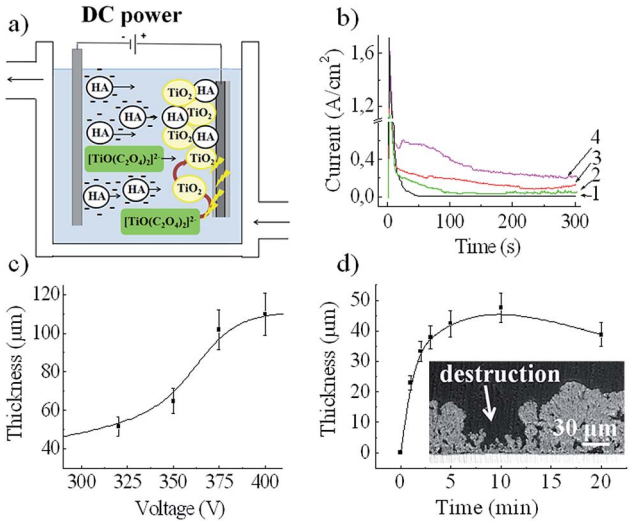

Fig. 1 (a) Scheme of the setup for PEO-EPD process. Electrodes titanium, electrolyte: 0.025 M $K_2[TiO(C_2O_4)_2]$, 0.025 M $Ca_3(C_6H_5O_7)_2$, 0.006 M $Ca_{10}(PO_4)_6(OH)_2$; (b) current time dependencies for PEO-EPD at 325 (1), 350 (2), 375 (3) and 400 V (4). (c) Thickness of oxide layer as a function of the applied voltage; (d) thickness of oxide layer as a function of deposition time during EPD process at 325 V. Insert shows SEM cross-sectional view of the TiO_2 layer after 20 min of PEO-EPD process.

coatings. It is visually seen that the application of the voltage higher than 320 V to the electrochemical cell results in the generation of yellow sparks. During the PEO process, the current transients are characterized by a decay of the current density from 1.6 to 0.05–0.07 A cm^{-2}, so that the higher voltage is applied, the more drastic is the current drop (Fig. 1b). Under high applied voltage ($U \geq 320$ V), within 10–150 s of the beginning of oxidation, the current density becomes almost invariable with time and the oxide film growth proceeds as a practically stationary process. At the applied voltage ranged from 320 to 400 V, an initial increase of the current changes to its further decay, which is due to the predominant passivating effect of the oxide coating formed in the interval of 25–150 s. It is clearly seen that at the PEO process, the greater is the voltage, the less is the value to which the current drops within a fixed time interval.

Uniform and smooth coatings are formed at 320 V with an average thickness of 40–45 μm (Fig. 1c). When the voltage increases up to 400 V, the thickness of the TiO_2 coating is three times larger. However, the formed coating starts to destruct due to dielectric breakdown. Thus, the optimal voltage for PEO process is 325–350 V.

The temporal evolution of the thickness during the PEO-EPD process at 320 V is shown in Fig. 1d. There is a significant increase in the thickness during the first 5 min of PEO process. Then the coating thickness becomes almost invariable with time. After 15 min of PEO process, the TiO_2 thickness begins to decrease. This may be associated with the loosening and partial destruction of the formed layer due to dielectric breakdown. This is also proved by mass decrease and SEM inspection of the coating (Fig. 1d, insert).

Morphology and composition of HA–TiO_2 coating

Fig. 2a shows Ti samples before and after PEO-EPD treatment in the electrolyte containing ethanol with a concentration of 20 vol%. It is evident that the PEO-EPD process leads to the formation of white or light-grey dense uniform coatings. The relative surface wettability of the coatings has been determined according to the water contact angle (Fig. 2a, insert). The wettability is found to depend on the applied voltage *via* PEO-EPD process. For example, the contact angle of HA–TiO_2 coating obtained at 325 V is 103.3° ± 5.2, while the contact angle of the coating prepared at $U \geq 350$ V is 4.3° ± 0.3. The contact angle of initial polished titanium is 70° ± 3.5. The hydrophobicity of the PEO-EPD coatings may be attributed to the formation of a hierarchical micro/nano-structure or a well-designed nanoporous structure.[26 28] The hydrophilicity could be explained by several factors: (i) changing the morphology of the PEO-EPD coatings obtained at voltage higher than 350 V and increasing its roughness and porosity.[29,30] At 400 V a bigger amount of gas released on the anode surface resulting in loosening and partial destruction of the PEO-EPD coating. (ii) When the voltage increases from 325 V to 400 V the PEO-EPD coatings become enriched with HA, which is known for its hygroscopicity[31 33] and ability to form super hydrophilic surfaces.[34 36]

Preliminary results have revealed that a highly porous uniform layer of TiO_2 forms by PEO treatment of titanium in the solution containing 0.025 M $K_2[TiO(C_2O_4)_2]$ and 0.025 M $Ca_3(C_6H_5O_7)_2$ at 320 V (Fig. 2b). The pores of the resultant coating are well separated and homogeneously distributed over the surface. The diameter of the pores varies from 0.5 to 2.5 μm. The coatings contain only Ti and O without any other elements as indicated by EDS.

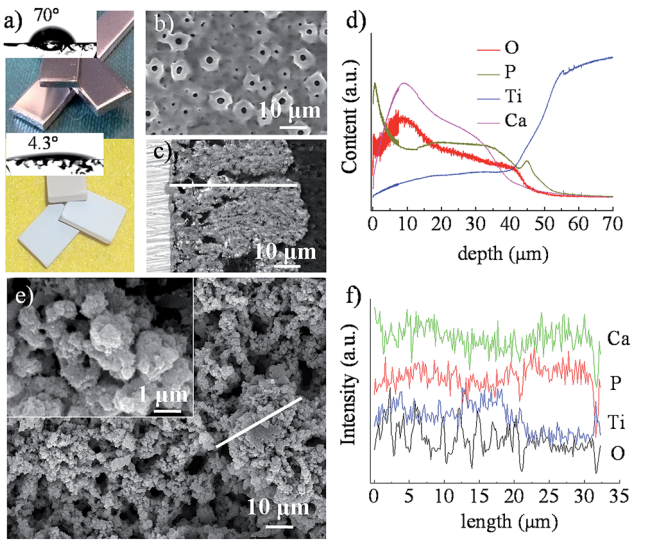

Fig. 2 (a) Images of the Ti samples before and after PEO-EPD treatment. Inserts show contact angle values; (b) SEM plan-view of the PEO treated coating; (c) SEM cross-sectional view of the PEO-EPD sample; (d) depth profile analysis of the PEO-EPD sample (element distribution on the cross of the coating was measured as shown by white line); (e) SEM plan-view images of the PEO-EPD treated samples; (f) element distribution on the plane of the PEO-EPD coating.

The PEO-EPD treatment of titanium changes drastically the morphology of the formed coatings (Fig. 2c, e and f). The coating is composed of roundish conglomerates with a size of 200–600 nm. Tiny HA and TiO_2 particles are observed on the surface, and some of the pores are clogged (Fig. 2e, insert). EDS analysis revealed the uniform distribution of Ca, P, Ti and O in a plane of the surface (Fig. 2f). The Ca/P ratio is 1.60 that is very close to the stoichiometric ratio of Ca/P in the HA (1.67).

The cross-section of the PEO-EPD coatings clearly shows the rough and porous structure of the HA–TiO_2 layer (Fig. 2c). Depth profile analysis of the PEO-EPD coatings confirms the presence of titanium and oxygen together with Ca and P in the bulk of the PEO-EPD coating (Fig. 2d). The data obtained prove that the TiO_2 and HA particles are simultaneously depositing on the Ti surface during the PEO-EPD process and coagulating into roundish conglomerates.

XRD patterns of the PEO-EPD coatings are shown in Fig. 3a. Peaks of the titanium (marked as Ti) substrate are observed on all the XRD patterns. The coatings formed by PEO of titanium in the solution containing 0.025 M $K_2[TiO(C_2O_4)_2]$ and 0.025 M $Ca_3(C_6H_5O_7)_2$ are composed of rutile (marked as R) and an equal amount of anatase (marked as A) (Fig. 3a, plot 1). The ratio of rutile/anatase content in the PEO-EPD coating does not depend on applied voltage.

After addition of HA suspension into electrolyte, peaks associated with HA (marked as HA) and tricalcium phosphate (in Fig. 3a marked as C) are detected along with rutile and anatase (Fig. 3a, curve 2). A small amount of tricalcium phosphate may be associated with a partial transformation of HA particles to tricalcium phosphate during the PEO process. It should be noted that the relative intensity of the HA peaks and the HA weight content increase with increasing the applied voltage, while the ratio of HA and TiO_2 phases changes insignificantly with the thickness increase in a range of 40–120 μm.

A FTIR spectrum of the PEO coating prepared in 0.025 M $K_2[TiO(C_2O_4)_2]$ + 0.025 M $Ca_3(C_6H_5O_7)_2$ at 320 V is shown in Fig. 3b (curve 1). The features at 3000–3750 cm^{-1} and 1300–1800 cm^{-1} in the as-deposited TiO_2 films show that there is a significant amount of water in the pores of the coating. The spectrum of the PEO-deposited TiO_2 coating exhibits a strong broad band in the region of 400–800 cm^{-1}, which can be assigned to the formation of Ti–O and Ti–O–Ti bonds. The broadening of the band related to Ti–O bond might be associated with an amorphous structure of the TiO_2 film due to incorporation of hydroxyl groups into the Ti–O bond network.[37,38] There are broad bands belonging to the OH^- and PO_4^{3-} groups of the HA in the PEO-EPD coating spectrum (curves 2 and 3, respectively). Characteristic peaks corresponding to PO_4^{3-} groups in HA (560–600 cm^{-1}, 961 cm^{-1}, 1030–1090 cm^{-1})[15,39] are visible in both spectra. The bands at 598 cm^{-1} (assigned to the deformation vibration of PO_4^{3-} ions) are shielded by broad bands of TiO_2.

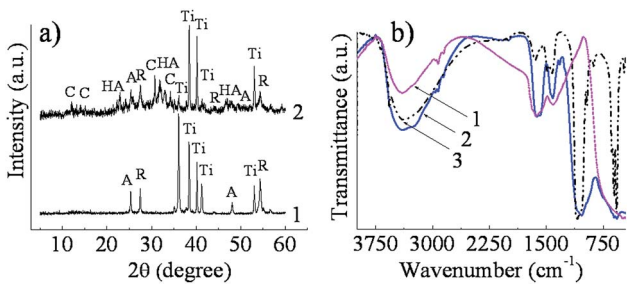

Fig. 3 XRD patterns (a) and FT-IR spectra (b) of the PEO-EPD samples obtained in the water ethanol electrolyte containing 0.025 M $K_2TiO(C_2O_4)_2$ and 0.025 M $Ca_3(C_6H_5O_7)_2$ without (1) and with (2) 0.006 M $Ca_{10}(PO_4)_6(OH)_2$, respectively. Crystalline HA powder was used as a standard (3).

Bioactivity test in SBF solution

Bioactivity of the obtained coatings is estimated by the apatite formation in SBF solution.[40–42] Fig. 4a illustrates the mass gain of the formed apatite on the PEO-EPD sample surface is in a range of 6–8%, while that on the PEO sample surface is approximately 2–3%. EDS analysis reveals an increase in the relative concentration of Ca and P in the PEO-EPD coatings after immersion in SBF for 21 days (Fig. 4b). SEM plan-view image of the PEO-EPD coatings after immersion in SBF solution for 21 days shows a thin rough apatite layer grown on the top of the coating while there is no apatite formation on the polished titanium substrate taken as a reference sample. As the amount of the formed apatite could indicate a high degree of bioactivity, the PEO-EPD coatings are expected to possess a higher bioactivity as compared with polished titanium and the PEO samples.

Tribological test

The wear rate of the PEO-EPD coating deposited at 320 V is 2.5 × 10^{-5} mm^3 N^{-1} m^{-1}, indicating a good wear resistance. It should be mentioned that the wear rate has increased from 1.9 × 10^{-4} mm^3 N^{-1} m^{-1} to 3.1 × 10^{-4} mm^3 N^{-1} m^{-1} with increasing the

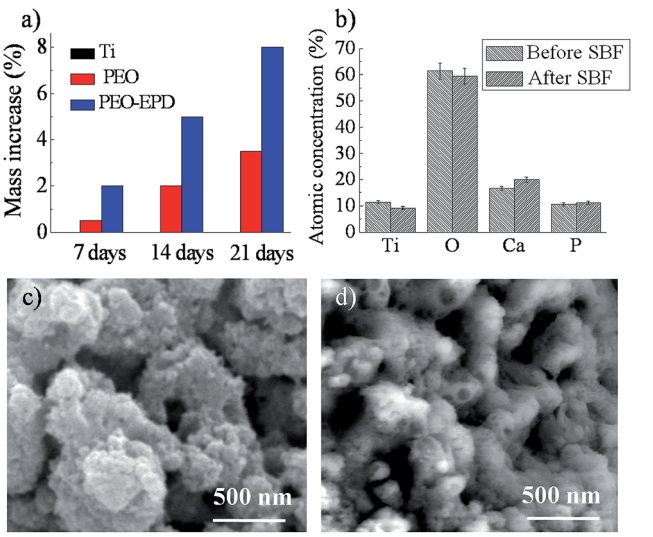

Fig. 4 Mass increase (a) and atomic concentration (b) of the PEO-EPD coatings after immersion in SBF solution for 7 21 days; SEM plan-view images of the PEO-EPD coating before (c) and after (d) their immersion in SBF solution for 21 days.

applied voltage during the PEO-EPD process. This fact may be related to an increase in the porosity and friability of the coating with increasing the applied voltage. The tribological tests have shown that the PEO-EPD coatings possess a good wear resistance. These coatings could be very prominent for biomedical applications.

Conclusions

The PEO-EPD process has been applied successfully to produce a bioactive HA–incorporated TiO_2 coating on the titanium surface in the electrolyte containing calcium citrate, potassium titanium(IV) oxalate and HA particles. The addition of ethanol to the electrolyte inhibits gaseous emission generated by the water electrolysis at the anode and allows the efficient incorporation of HA particles into the TiO_2 coating during the PEO-EPD process. The surface morphology and microstructure of the coating can be affected considerably by the applied voltage. The amount of the deposited HA can be enhanced by increasing the applied voltage. The PEO-EPD coatings induce a precipitation of apatite in SBF solution. These coatings are revealed to have a good wear resistance and could be very promising for biomedical applications.

Acknowledgements

Authors thank Maksim Starykevich (Department of Materials and Ceramics Engineering, CICECO, University of Aveiro) for help in the laboratory and providing protocols.

Notes and references

1 D. M. Brunette, P. Tengvall, M. Textor and P. Thomsen, *Titanium in medicine*, Springer Verlag, Berlin, 2001.
2 L. H. Li, Y. M. Kong, H. W. Kim, Y. W. Kim, H. E. Kim, S. J. Heo and J. Y. Koak, *Biomaterials*, 2004, **25**, 2867.
3 E. V. Skorb and D. V. Andreeva, *Adv. Funct. Mater.*, 2013, **23**, 4483.
4 H. Kurzweg, R. B. Heimann and T. Troczynski, *Biomaterials*, 1998, **19**, 1507.
5 H. Ishizawa and M. Ogino, *J. Biomed. Mater. Res.*, 1995, **29**, 65.
6 A. L. Yerokin, X. Nie, A. Leyland, A. Matthews and S. J. Dowey, *Surf. Coat. Technol.*, 1999, **122**, 73.
7 Y. Han, S. H. Hong and K. Xu, *Mater. Lett.*, 2002, **56**, 744.
8 O. O. V. der Biest and L. J. Vandeperre, *Annu. Rev. Mater. Res.*, 1999, **29**, 327.
9 O. Albayrak, O. El-Atwani and S. Altintas, *Surf. Coat. Technol.*, 2008, **202**, 2482.
10 K. Grandfield, F. Sun, M. FitzPatrick, M. Cheong and I. Zhitomirsky, *Surf. Coat. Technol.*, 2009, **203**, 1481.
11 W. Jarernboon, S. Pimanpang, S. Maensiri, E. Swatsitang and V. Amornkitbamrung, *J. Alloys Compd.*, 2009, **476**, 840.
12 I. Singh, C. Kaya, M. S. P. Shaffer, B. C. Thomas and A. R. Boccaccini, *J. Mater. Sci.*, 2006, **41**, 8144.
13 X. Nie, A. Leyland and A. Matthews, *Surf. Coat. Technol.*, 2000, **125**, 407.
14 S. H. Lee, H. W. Kim, E. J. Lee, L. H. Li and H. E. Kim, *J. Biomater. Appl.*, 2006, **20**, 195.
15 Y. Bai, I. S. Park, S. J. Lee, T. S. Bae, W. Duncan, M. Swain and M. H. Lee, *Appl. Surf. Sci.*, 2011, **257**, 7010.
16 Y. Bai, K. A. Kim, I. S. Park, S. J. Lee, T. S. Bae and M. H. Lee, *Mater. Sci. Eng., B*, 2011, **176**, 1213.
17 D. Y. Kim, M. Kim, H. E. Kim, Y. H. Koh, H. W. Kim and J. H. Jang, *Acta Biomater.*, 2009, **5**, 2196.
18 L. H. Li, H. W. Kim, S. H. Lee, Y. M. Kong and H. E. Kim, *J. Biomed. Mater. Res., Part A*, 2005, **73**, 48.
19 M. S. Kim, J. J. Ryu and Y. M. Sung, *Electrochem. Commun.*, 2007, **9**, 1886.
20 J. H. Ni, Y. L. Shi, F. Y. Yan, J. Z. Chen and L. Wang, *Mater. Res. Bull.*, 2008, **43**, 45.
21 Y. Li, I. S. Lee, F. Z. Cui and S. H. Choi, *Biomaterials*, 2008, **29**, 2025.
22 E. Matykina, R. Arrabal, P. Skeldon and G. E. Thompson, *Acta Biomater.*, 2009, **5**, 1356.
23 S. A. Ulasevich, V. K. Krut'ko, O. N. Musskaya, A. I. Kulak, L. A. Lesnikovich and T. V. Safronova, *Russ. J. Appl. Chem.*, 2013, **86**, 146.
24 T. Kokubo and H. Takadama, *Biomaterials*, 2006, **27**, 2907.
25 S. Lebrette, C. Pagnoux and P. Abelard, *J. Eur. Ceram. Soc.*, 2006, **26**, 2727.
26 L. Feng, Y. Zhang, J. Xi, Y. Zhu, N. Wang, F. Xia, L. Jiang and L. Petal, *Langmuir*, 2008, **24**, 4114.
27 Y. Lai, X. Gao, H. Zhuang, J. Huang, C. Lin and L. Jiang, *Adv. Mater.*, 2009, **21**, 3799.
28 M. A. Henderson, *Langmuir*, 1996, **12**, 5093.
29 F. Rupp, L. Scheideler, D. Rehbein, D. Axmann and J. Geis-Gerstorfer, *Biomaterials*, 2004, **25**, 1429.
30 M. Lampin, R. Warocquier-Clérout, C. Legris, M. Degrange and M. F. Sigot-Luizard, *J. Biomed. Mater. Res.*, 1997, **36**, 99.
31 C. Santos, R. L. Clarke, M. Braden, F. Guitian and K. W. M. Davy, *Biomaterials*, 2002, **23**, 1897.
32 M. F. Hsieh, L. H. Perng, T. S. Chin and H. G. Perng, *Biomaterials*, 2001, **22**, 2601.
33 S. Deb, M. Braden and W. Bonfield, *Biomaterials*, 1995, **16**, 1095.
34 W. K. Yeung, G. C. Reilly, A. Matthews and A. Yerokhin, *J. Biomed. Mater. Res.*, 2013, **101**, 939.
35 N. Eliaz, S. Shmueli, I. Shur, D. Benayahu, D. Aronov and G. Rosenman, *Acta Biomater.*, 2009, **5**, 3178.
36 Y. Okabe, S. Kurihara, T. Yajima, Y. Seki, I. Nakamura and I. Takano, *Surf. Coat. Technol.*, 2005, **196**, 303.
37 M. J. Alam and D. C. Cameron, *J. Sol-Gel Sci. Technol.*, 2002, **25**, 137.
38 C. Y. Wang, H. Groenzin and M. J. Shultz, *J. Phys. Chem. B*, 2004, **108**, 265.
39 A. Ghicov, S. P. Albu, R. Hahn, D. Kim, D. T. Stergiopoulos, J. Kunze and C. A. Schiller, *J. Phys. Chem.*, 2008, **112**, 12687.
40 C. Ohtsuki, T. Kokubo and T. Yamamuro, *J. Non-Cryst. Solids*, 1992, **143**, 84.
41 T. Kokubo, H. M. Kim and M. Kawashita, *Biomaterials*, 2003, **24**, 2161.
42 T. Kokubo, *Acta Mater.*, 1998, **46**, 2519.